Vol. **130** (2016) *ACTA PHYSICA POLONICA A* No. 4

Proceedings of the XXIII Conference on Applied Crystallography, Krynica Zdrój, Poland, September 20–24, 2015

Crystallography and Morphology of Chromium Rich Eutectic Carbides in an As-Cast Fe–Cr–C Alloy Crystallized in Non-Equilibrium Conditions

K. Wieczerzak[a,*], P. Bała[a,b], T. Tokarski[b] and M. Gajewska[b]

[a]AGH University of Science and Technology, Faculty of Metals Engineering and Industrial Computer Science,
al. A. Mickiewicza 30, 30-059 Krakow, Poland

[b]AGH University of Science and Technology, Academic Centre for Materials and Nanotechnology,
al. A. Mickiewicza 30, 30-059 Krakow, Poland

The crystallography and microstructure of eutectic carbides crystallizing in non-equilibrium conditions in hypoeutectic Fe24Cr0.8C have been studied by light microscopy, scanning electron microscopy, and transmission electron microscopy. The alloy was synthesized in an arc furnace in high purity argon atmosphere and crystallized on water-cooled copper mould. Greater thermal gradient in regions close to water-cooled, copper mould in comparison with top of the ingot gives a formation of eutectic carbides with two morphologies: large polygonal carbides and surrounding them much smaller, plate-like carbides instead of rod-like carbides, observed in top of the ingot. There was no evidence for influence of non-equilibrium crystallization to the formation of types of carbides different than $M_{23}C_6$.

DOI: 10.12693/APhysPolA.130.1007

PACS/topics: 81.20.–n, 81.30.Fb, 81.70.–q

1. Introduction

Alloys from the Fe–Cr–C system are widely used in applications, where erosion, abrasion, and corrosion resistance are necessary. Their attractive physicochemical and mechanical properties result from presence of hard carbides and toughness matrix enriched in chromium, which allows to form protective oxide layer on the surface. The wear resistance of alloys from the Fe–Cr–C system might be controlled by volume fraction of eutectic carbides, their type, morphology and orientation [1–4]. Generally, the main factors affecting these parameters are chemical composition, including varying the Cr/C ratio, and solidification conditions [3, 5–7]. Depending on the Cr/C ratio three types of microstructures are possible such as hypoeutectic, eutectic, and hypereutectic strengthened by the cementite M_3C, M_7C_3 and $M_{23}C_6$ complex carbides, where M is Cr and Fe [5, 6, 8–13]. For equilibrium conditions phase composition might be predicted using Fe–Cr–C phase diagram. Nonetheless, such conditions in industrial practice are seldom achieved. Fras et al. [3] showed that for increasing crystal growth rates the fiber spacing of unidirectionally solidified Fe–Cr–C decreases linearly. Consequently, with the increase in growth rate and decrease in fiber spacing an increase in tensile strength of the alloy is observed. Inoue and Masumoto [7] showed that in irons containing 18 wt% Cr and 3 to 8 wt% tungsten or molybdenum the formation of eutectic M_7C_3 and $M_{23}C_6$ might be suppressed by extremely rapid cooling to produce microstructure containing a very fine mixture of austenite and M_3C. The M_3C is softer than e.g. M_7C_3 [6] and its appearance might have a significant effect on the mechanical and physicochemical properties. Imurai et al. [14] showed that in 28 wt% chromium, hypoeutectic irons containing 0 to 10 wt% molybdenum the reduction of the carbide-matrix hardness difference, the increase of macro-hardness, and the increase of matrix corrosion resistance affect on improving erosion-corrosion resistance. Studies on the type and morphology characterization of the eutectic carbides in Fe–Cr–C alloys are important from the point of view of manufacturing and design of new materials based on this system.

In the present work the hypoeutectic Fe24Cr0.8C alloy was synthesized during non-equilibrium conditions. In previous work [12], the authors demonstrated that solidification rate, which is a function of thermal gradient, has a significant impact on the size and morphology of eutectic carbides in hypoeutectic Fe–Cr–C alloy. Similar observations were reported by Doğan et al. [10] in hypereutectic Fe–Cr–C alloy containing 26 wt% Cr. They found that in microstructure in regions near the mould wall, where the undercooling is greater, more rod-shaped carbides in comparison with the interior of the casting are observed.

The aim of the study was to characterize morphology and type of carbides in investigated alloy in regions close to water-cooled, copper mould.

2. Experimental details

The material for investigations was synthesized by arc melting process, under argon atmosphere using an Arc Melter AM (Edmund Bühler GmbH). For process mixture of high purity (> 99.9%) elements such as chromium and iron with Fe–C alloy (with known carbon content)

---

*corresponding author; e-mail: kwiecz@agh.edu.pl

were used. The charge was melted on a water-cooled, copper mould. Consequently, the ingot with mass of approximately 35 g was obtained. The chemical composition analysis was performed on the cross-section of the ingot with with optical emission spectrometer Foundry-Master (WAS). Based on five measurements an average value and standard deviation for each element were calculated. Results are summarized in Table I.

TABLE I

Chemical composition of the Fe–Cr–C alloy [wt%].

C	Si	Mn	Cr	P	S	Fe
0.79	0.20	0.12	24.47	0.005	0.009	
±	±	±	±	±	±	bal.
0.14	0.03	0.01	0.46	0.002	0.003	

Microstructures were examined on Nikon LV150N light microscope (LM) and FEI VERSA 3D scanning electron microscope (SEM), equipped with the Apollo XP SDD energy dispersive spectroscopy (EDS) detector. Maps of chemical distribution and quantitative analysis were obtained under accelerating voltage of 30 kV and current of 8 nA. Microstructural observations were carried out on the samples after polishing and etching. The etching agent was composed of 30 g NH_4F, 50 ml HNO_3 and 20 ml H_2O.

The TEM investigations and analysis of the chemical distributions (X-ray mapping) in uncovered phases was carried out on TEM lamella. The lamella was prepared from the ingot in region close to the copper mould. The TEM specimen was performed by conventional cutting, grinding and ion-milling using a FEI QUANTA 3D 200i system. The TEM experiment was carried out on FEI TECNAI TF 20 X-TWIN electron microscope, equipped with a field emission electron gun (FEG) operated at 200 kV.

3. Results and discussion

Figure 1 shows microstructure of the Fe–Cr–C ingot in regions close to the copper mould. There are visible irregular, quasi equiaxed crystals of Fe–Cr solid solution and eutectic carbides in interdendritic zones (Fig. 1a,b). In these regions crystals nucleated and grew in a very short time. Figure 1c and d shows morphology of eutectic carbides. As it can been seen eutectic carbides exhibit two characteristic morphologies. It is easy to distinguish large polygonal eutectic carbides, which are surrounded by much smaller eutectic carbides with predominantly plate-like morphology (see Fig. 1d). Regions surrounding eutectic carbides are depleted in chromium, therefore they are more sensitive to etching agent. During solidification solubility of chromium and carbon in the matrix decreases with temperature. Simultaneously eutectic carbides, formed in the previous stage, become nuclei for further carbide deposition. The supersaturation is reduced by solid state diffusion from the matrix to the interfacial boundaries, but only over a distance approximately equal to the diffusion length. It is a reason why the carbides, formed at the beginning, on the boundary between eutectic and matrix exhibit greater thicknesses in comparison with carbides formed during further eutectic reaction. It might be assumed that for formation of eutectics with different morphology there is responsible segregation of alloy elements and their partitioning coefficients.

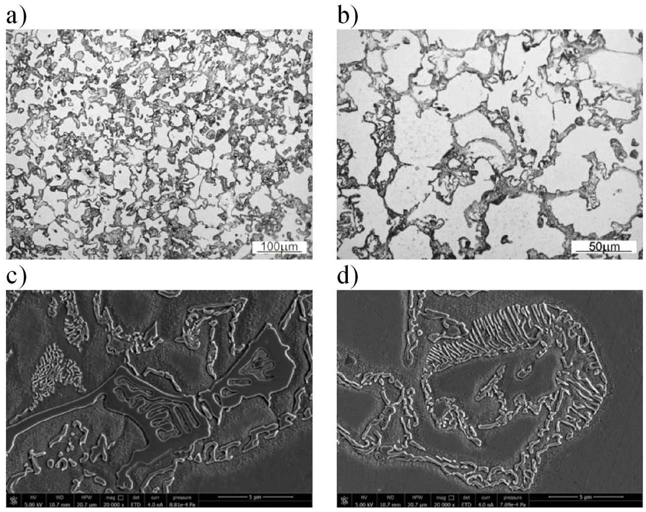

Fig. 1. Microstructure of investigated alloy in regions close to the copper mould: (a,b) light microscope, (c,d) SEM–SE (SE — secondary electrons).

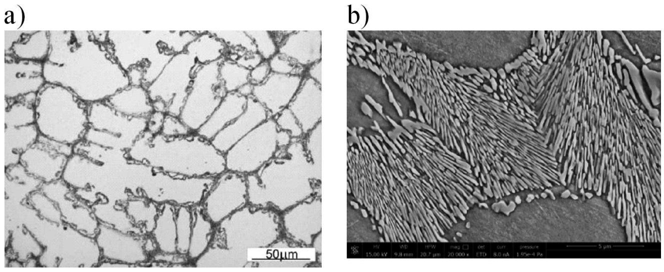

Fig. 2. Characteristic morphology of eutectic carbides, observed in top of the ingot.

The typical morphology of eutectic carbides, observed in the top of the ingot is shown in Fig. 2. Dendrites in these region have equiaxed shapes, because their latent heat is extracted radially through the undercooled melt. As a consequence, thermal gradient in these regions is much smaller in comparison with regions close to the copper mould, which causes formation of rod-like eutectic carbides. Wiengmoon [6] emphasizes that sometimes cross-sections of fine eutectic carbides are incorrectly described as globular.

Figure 3 shows X-ray maps chemical distribution of Cr and Fe in eutectic carbides and matrix. As it can been seen, eutectic carbides are enriched in Cr, which exhibit greater affinity to carbon than Fe [15]. Figure 2c shows bright-field (BF) TEM micrograph of analysed region. The darker appearance of carbides results from the strong diffraction from their crystallographic planes.

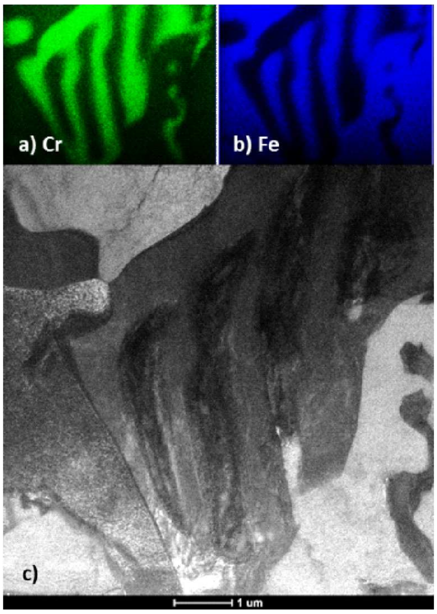

Fig. 3. Maps of chemical distribution (SEM–EDS) in eutectic carbides: (a) Cr, (b) Fe, and bright-field TEM micrograph of analysed region.

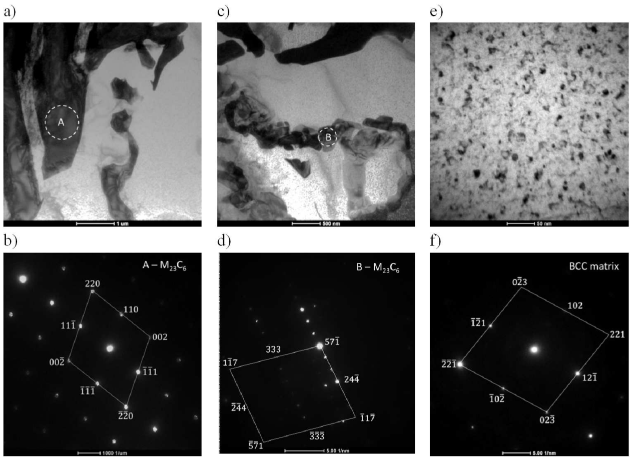

Fig. 4. A BF-TEM micrographs (a,b,c) with corresponding SAD patterns (b,d,f): (a) morphology of large polygonal eutectic carbides, (b) the SAD pattern from region A, (c) morphology of smaller eutectic carbides surrounding aforementioned carbides, (d) the SAD pattern from region B, (e) morphology of secondary carbides precipitated in matrix, (f) the SAD pattern from matrix.

The electron-probe microanalysis (EPMA) revealed that matrix contains about 23 wt% of Cr. Based on carbon and chromium content in the alloy and results presented by Khvan et al. [9], focused on thermodynamic analysis of the Fe–Cr–C system, in equilibrium conditions the appearance of $M_{23}C_6$ carbides in the Fe24Cr0.8C alloy might be expected.

Figure 4 shows morphologies of observed phases in Fe–Cr–C alloy with corresponding selective area diffraction (SAD) patterns. It was found that both types of carbides are $M_{23}C_6$ (space group $Fm\bar{3}m$). It seems that in investigated alloy the $M_{23}C_6$ carbides are thermodynamically stable and their formation was not supressed by high undercooling, obtained during experiment. Nevertheless solidification conditions have significant influence to their morphology. Simultaneously it was found that during cooling, the supersaturation was high enough to homogeneous precipitation of secondary carbides with few nm in diameter. Matrix of the alloy has bcc crystal structure.

4. Conclusions

In the present work the hypoeutectic alloy from Fe–Cr–C system, containing 0.79 wt% C and 24 wt% Cr, was synthesized. It was found that during non-equilibrium crystallization the thermal gradient and solidification rate have significant influence on the morphology of eutectic carbides. Greater thermal gradient in regions close to water-cooled, copper mould in comparison with top of the ingot gives a formation of eutectic carbides with two morphologies: large polygonal carbides and surrounding them much smaller, plate-like carbides instead of rod-like carbides, observed in top of the ingot. There was no evidence for influence of non-equilibrium crystalization to the formation of types of carbides different than $M_{23}C_6$.

References

[1] A. Wiengmoon, J.T.H. Pearce, T. Chairuangsri, *Mater. Chem. Phys.* **125**, 739 (2011).

[2] Ö.N. Dogan, J.A. Hawk, *Wear* **189**, 136 (1995).

[3] E. Fras, E. Guzik, H.F. Lopez, *Metall. Trans. A* **19**, 1235 (1988).

[4] J.J. Coronado, *Wear* **270**, 823 (2011).

[5] G.L.F. Powell, R.A. Carlson, V. Randle, *J. Mater. Sci.* **29**, 4889 (1994).

[6] A. Wiengmoon, *Naresuan Univ. Eng. J.* **6**, 64 (2011).

[7] A. Inoue, T. Masumoto, *Metall. Trans. A* **11**, 739 (1980).

[8] M. Venkatraman, J.P. Neumann, *Bull. Alloy Phase Diagrams* **11**, 152 (1990).

[9] A.V. Khvan, B. Hallstedt, C. Broeckmann, *Calphad Comput. Coupling Phase Diagrams Thermochem.* **46**, 24 (2014).

[10] Ö.N. Doğan, J.A. Hawk, G. Laird, *Metall. Mater. Trans. A* **28**, 1315 (1997).

[11] D.M. Kundrat, M. Chochol, J.F. Elliott, *Metall. Trans. B* **15**, 663 (1984).

[12] K. Wieczerzak, P. Bała, M. Stępień, G. Cios, T. Kozieł, *Arch. Metall. Mater.* **60**, 769 (2015).

[13] C.M. Chang, Y.C. Chen, W. Wu, *Tribol. Int.* **43**, 929 (2010).

[14] S. Imurai, C. Thanachayanont, J.T.H. Pearce, T. Chairuangsri, *Arch. Metall. Mater.* **60**, 919 (2015).

[15] H.J. Goldschmidt, in: *Interstitial Alloys*, Springer Science + Business Media, LLC, New York 1967, p. 88.